

Electrolyte concentration effects on Zn-Cu galvanic cells: Powering LEDs through redox optimisation

Anastasiia Danshyna^a, Grace Mihaljevic^a, Stefano Furlan^a, Isaac Sleath^a, Alexander Palmer^a, Jordan Kambanis^a, Masoomeh Asghar Nejad-Laskoukalayeh^a, Benedict Tai^a, David Alam^a, Thomas A Whittle^a, Gobinath Rajarathnam^a.

^a School of Chemical and Biomolecular Engineering, The University of Sydney, Sydney, NSW, 2006, Australia

ARTICLE INFORMATION

ABSTRACT

Keywords: Battery, Electrochemistry, Energy Storage, Galvanic Cell, Redox Reactions

This study investigated the effect of electrolyte concentration on the performance of Zn-Cu galvanic cells and their ability to power LEDs with different voltage requirements. Three half-cells were constructed using Zn and Cu electrodes, each immersed in electrolyte solutions of different molarities. Each configuration was tested individually and in series to assess voltage output and LED activation. Results showed that higher molarity solutions produced slightly higher voltages, and connecting cells in series increased total voltage. While single cells could not power any LEDs, series connections of two and three cells successfully powered low- and high-threshold LEDs, respectively. These findings highlight key redox and electrochemical principles relevant to practical energy applications. Electrochemical systems based on similar reactions are essential in medical implants, electric vehicles, and next-generation energy storage technologies, where efficient and reliable power delivery is at the heart of these applications.

1. Introduction

Electrochemical systems based on aqueous zinc (Zn) chemistry have gained renewed attention due to their inherent safety, material abundance, low toxicity, and adaptability to diverse cell configurations [1]-[3]. Among these, the classical zinc-copper (Zn-Cu) galvanic cell remains one of the most recognisable and instructive configurations in both pedagogical and exploratory electrochemistry. Originally conceptualised in the early 19th century, this system played a foundational role in shaping the understanding of redox processes and battery operation [4]. Today, while its role as a commercial power source has diminished, the Zn-Cu cell continues to offer significant value for educational experimentation, laboratory-scale power generation, and as a benchmark system for understanding the influence of electrolyte and cell design variables on electrochemical performance [5].

The operation of the Zn-Cu cell is governed by the redox couple Zn^{2+}/Zn at the anode and Cu^{2+}/Cu at the cathode, producing a theoretical open-circuit voltage in the range of 0.5 to 1.5 V direct current (dc) under standard conditions [6]. While the basic electrochemical pathway has remained unchanged for over two centuries, advances in electrode materials, separator technologies, and electrolyte formulation have improved the understanding of how to modulate and optimise galvanic-cell behaviour [7]. These improvements are particularly relevant as simple redox pairs re-emerge in next-

generation aqueous systems such as zinc-bromine flow batteries and hybrid zinc-ion devices [8].

Historically, the Daniell cell -an archetypal Zn-Cu configuration introduced in 1836- addressed earlier limitations of hydrogen evolution and electrode passivation by employing separate electrolyte compartments and a porous barrier [4]. This conceptual separation of ionic environments remains critical in contemporary flow-battery and hybrid electrochemical systems.

The electrolyte concentration plays a dual role: it directly influences the cell potential via the Nernst equation and indirectly governs the ionic conductivity and mass transport [9]. This paper focuses on quantifying how variations in zinc sulphate (ZnSO_4) and copper sulphate (CuSO_4), molarity affects open-circuit voltage, discharge power, and light-emitting diodes (LED)-driving capability with the series wiring topology, which is commonly used in electrical engineering practices in battery cell connections.

The aim of this paper is to systematically evaluate the impact of electrolyte concentration and cell configuration on the performance of laboratory-scale Zn-Cu galvanic cells.

The objectives are twofold; firstly, to quantify the relationship between electrolyte molarity (0.5-1.5 mol/L) and dc voltage, current, and power output. The second goal is to compare three practical cell-stack configurations with series-

only electrical connection, in their ability to power small devices such as LEDs.

The remainder of this paper is organised as follows: Section 2 describes the materials, concentrations, and electrical configurations tested. Section 3 presents the experimental results, including voltage, current and power parameters with LED forward dc voltage activation thresholds. Section 4 discusses the implications of these results in the context of galvanic-cell optimisation and redox-battery design in the context of chemical engineering. Section 5 offers concluding remarks and outlines future directions, particularly for scaling up Zn-Cu cells for niche applications and enhancing their educational utility through data-driven design tools.

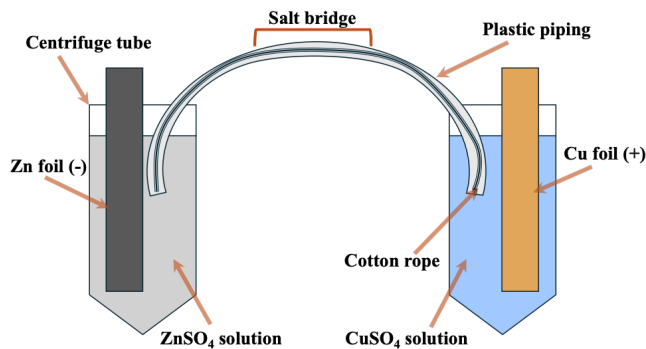


Figure 1. Zn-Cu galvanic half-cell schematic.

2. Methodology

2.1 Experimental design

This study investigated the influence of electrolyte concentration on the performance of zinc–copper galvanic cells. Each cell was constructed using Zn and Cu electrodes immersed in ZnSO₄ and CuSO₄ solutions, respectively. Electrolyte concentrations were systematically varied from 0.5 M to 2.0 M to assess their effect on open-circuit voltage (V_{oc}), short-circuit current (I_{sc}), and the cell’s capacity to power LEDs. Measurements were recorded under both open-circuit and short-circuit conditions. Cells were tested as single units and in series and parallel configurations. LEDs with varying forward voltage thresholds were used to evaluate practical power output, P_{dc} (1). The materials and equipment used in this experiment are listed in Table 1.

$$P_{dc} = V_{dc} \times I_{dc}, [W] \tag{1}$$

where V_{dc} I_{dc} – dc voltage and current of the battery (connected galvanic cells).

$$E_j = P_{dc} \times t, [J] \tag{2}$$

E_j is the energy output, determined as a product of power P_{dc} and time t in seconds. Similarly, the specific energy per volume:

$$E_{js} = \frac{E_j}{Vol}, [J] \tag{3}$$

where E_j – energy output and Vol – is the volume of the electrolyte.

Table 1

List of materials used in the investigation.

Equipment	Quantity	Parameter
Zn foil strips ¹	3	6 cm
Cu foil strips ²	3	6 cm
Aqueous ZnSO ₄ solution ³	60 mL	2.0 mol/L
Aqueous CuSO ₄ solution ⁴	60 mL	2.0 mol/L
Aqueous KCl solution ⁵	5	2.0 mol/L
Deionised water	120 mL	
Cotton ropes	3	≈20 cm
U-shaped plastic pipe lengths	3	≈20 cm
Centrifuge tubes	6x 50 mL	
Dual-ended wired alligator clips	4	
Digital multimeter	1	
LED lights in colours green, blue, white, yellow, red	6	
Beaker	100 mL	
Measuring cylinder	100 mL	
Plastic pipettes	2	
Test tube rack	1	
Electronic stopwatch	1	

2.2 Cell Assembly

The necessary equipment was gathered, and 3 lengths of cotton rope were submerged in a beaker containing 50 mL of 2.0 mol/L aqueous KCl solution. The 100 mL measuring cylinder and a plastic pipette were used to create 3 centrifuge tubes of varying concentrations for each electrolyte according to the volumes listed in Table 2.

Table 2

Required volumes for electrolyte solutions of varying concentrations.

Electrolyte Concentration (mol/L)	Volume of electrolyte solution required (mL)	Volume of deionised water required (mL)
0.5	10	30
1	20	20
1.5	30	10

¹ Zinc Sheet (Chem Supply – TG 0.1 mm thick) [ZT006-500G]

² Copper metal foil (Chem Supply – LR 0.1 mm thick) [CL054-500G]

³ Zinc sulfate heptahydrate (Chem Supply - AR grade) ZA012-500G

⁴ Copper (II) sulphate pentahydrate (Univar, AR, AJA171-500G)

⁵ Potassium chloride (Univar, AR, AJA383-500G)

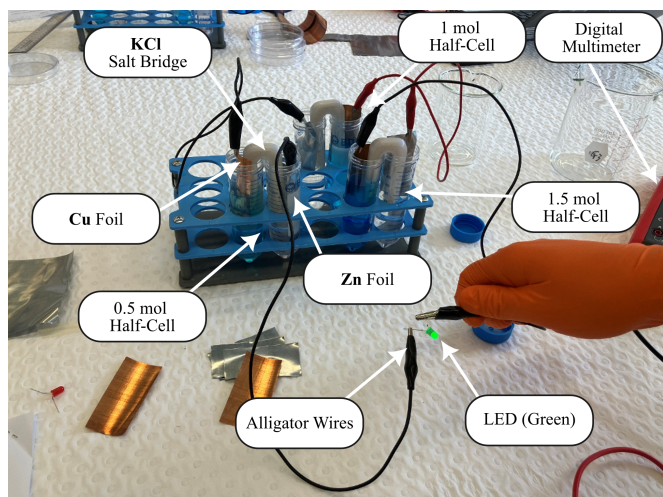


Figure 2. Photograph of experimental set-up for the half-cell series, seen with 3 half-cells illuminating the green LED.

The 3 saturated lengths of cotton rope were removed from the KCl solution and threaded through the 3 lengths of U-shaped plastic piping, to create 3 salt bridges for the half-cells. The 6 centrifuge tubes were arranged in pairs in the test tube rack, with a centrifuge tube containing ZnSO₄ solution placed adjacent to the centrifuge tube containing CuSO₄ solution of the same concentration. The centrifuge tube pairs, Zn foils, Cu foils, and salt bridges were set up creating 3 galvanic half-cells with electrolyte concentrations of 0.5, 1, and 1.5 mol/L. The foils were submerged ≈ 1/3 of the way into the electrolyte solution, mirroring the setup outlined in Figure 1.

2.3 Measurement protocol

The electronic multimeter was used to measure the voltage and current of each half-cell using two alligator clips which connected the positive terminal of the multimeter to the Cu foil and the negative terminal of the multimeter to the Zn foil. The results were recorded.

Table 3

Raw voltage, current, and LED data for each half-cell configuration.

Half-Cell Configuration	Theoretical Voltage, (V)	Voltage, (V)	Current, (mA)	LED Light Illumination Observed				
				Red	Yellow	White	Blue	Green
Single half-cell, (0.5 mol/L concentration)		1.075	1.43	X	X	X	X	X
Single half -cell, (1 mol/L concentration)	1.101 ¹	1.076	1.411	X	X	X	X	X
Single half-cell, (1.5 mol/L concentration)		1.077	1.315	X	X	X	X	X
2 half-cells in series, (0.5 and 1 mol/L concentrations)	2.2	2.075	1.117	✓	X	X	X	X
2 half-cells in series, (1 and 1.5 mol/L concentrations)		2.145	1.538	✓	X	X	X	X
3 half-cells in series, (0.5, 1, and 1.5 mol/L concentrations)	3.3	3.188	1.671	✓	✓	✓	✓	✓

For each half-cell the free ends of the alligator clips were clipped onto the metal legs of the red LED to test whether the half-cell was able to light up the LED. If the LED did light up, it was allowed to glow for 3 seconds, measured with the stopwatch. Observations were recorded. (Note: other LED colours were not tested as they required higher voltages and currents than the red LED).

The following half-cell series were assembled by connecting the Zn foil of one to the Cu foil of the next using alligator wires; 0.5 and 1 mol concentrations, 1 and 1.5 mol concentrations, and 0.5, 1, and 1.5 concentrations. The process of voltage and current measurement was repeated for each configuration, and the results were recorded. The red, white, yellow, blue, and green LEDs were tested for each configuration using the same method as outlined above, and the results and observations were recorded.

3. Results

3.1 Analysis of galvanic cell performance: Influence of electrolyte concentration and cell configuration.

The results clearly demonstrate how both electrolyte concentration and cell configuration influence the output of Zn-Cu galvanic cells, as presented in Table 2. According to electrochemical theory, especially the Nernst equation (4), increasing the concentration of ions in solution increases the electrode potential.

This was evident in the data: although all single-cell setups showed similar theoretical voltages (~1.1 V), those with higher molarity showed slightly higher measured voltages and current-as you can see in Figure 4.

$$E_e = E^\circ - \frac{RT}{nF} \ln Q \tag{4}$$

where E° – is standing electrode potential, R – universal gas constant, T – temperature (K), n – number of electrons transferred, F – Faraday’s constant, and Q – is the reaction quotient.

Table 4

Calculated output and specific power and energy for each half-cell configuration.

Half-Cell Configuration	Electrolyte Volume, (mL)	Submerged Electrode Area, (cm ²)	LED illumination time, (s)	Power Output, (mW)	Specific Power, (mW/cm ²)	Energy Output, (mJ)	Specific Energy (mJ/mL)
Single half-cell, (0.5 mol/L concentration)			-	1.538	0.256	-	-
Single half -cell, (1 mol/L concentration)			-	1.519	0.253	-	-
Single half-cell (1.5 mol/L concentration)	40	6	-	1.417	0.236	-	-
2 half-cells in series (0.5 and 1 mol/L concentrations)				2.318	0.386	6.954	0.174
2 half-cells in series (1 and 1.5 mol/L concentrations)			3	3.3	0.55	9.9	0.248
3 half-cells in series (0.5, 1, and 1.5 mol/L concentrations)				5.327	0.889	15.981	0.4

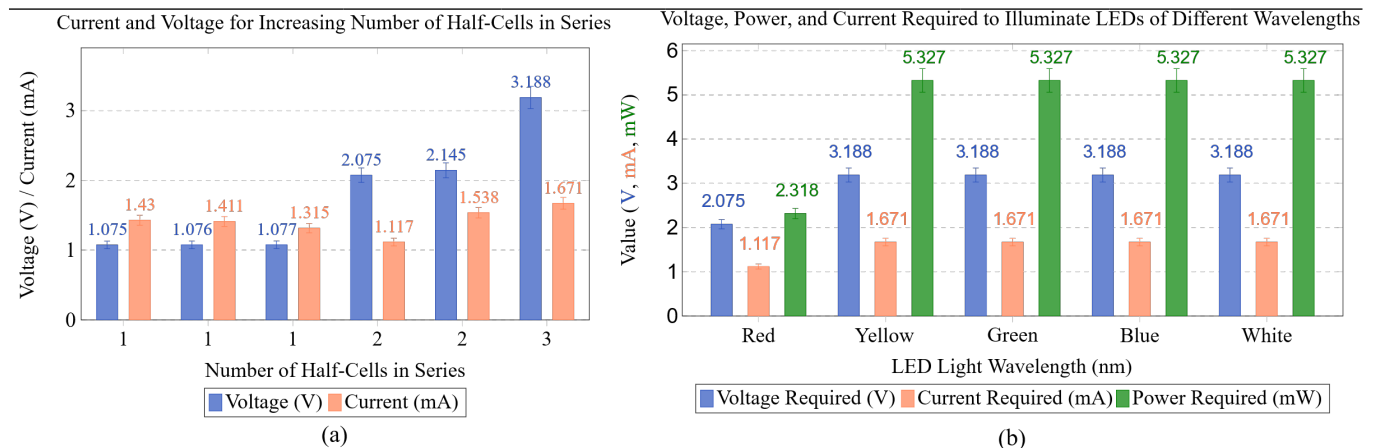


Figure 3. Experimental results: electrical parameters of series connected half-cells. (a) Voltage and current by cell configuration, (b) comparison of LED voltage thresholds to switch on the LED and half-cell dc power output.

None of the single cells produced enough power to illuminate any LEDs. In contrast, two cells in series powered the red LED, and three cells powered all LEDs, refer to Table 2 and Figure 3(b). This confirmed the theoretical prediction that series connections increase total voltage of the connected half-cells, whilst keeping the same dc current flow, albeit with some variations due to the cable resistance change and imperfect connection of alligator wires, as shown in Figure 3(a). Furthermore, the linear relationship with the increasing number of half-cells (i.e. total series dc voltage) and total power delivered to LED can be observed Table 3. From chemical perspective, higher electrolyte concentration and series configurations yielded higher energy output, so that various half-cells configurations and connection can results in

different voltage-current output from the resultant battery system.

During the work only one measurement per LED was performed, hence the error bars are established using an assumed fixed uncertainty, rather than a statistical deviation. In this work, 5% deviation was utilised to estimate the possible measurements errors and error bars in Figure 3, as per (5). Instead, the error bars were created using an assumed percentage uncertainty, specifically:

$$\Delta X_i = 0.05 \times x_i, \tag{5}$$

where x_i – is the measurement (i.e. voltage and current).

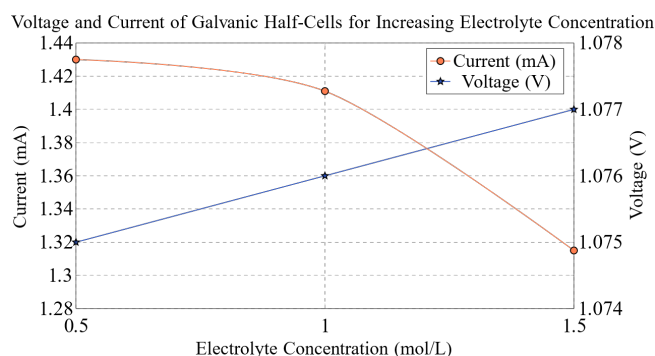


Figure 4. Voltage and current across different electrolyte concentrations.

4. Discussion

4.1 Relationship between results and theory of voltage

This investigation into Zn-Cu galvanic cells provides valuable insights into electrochemical principles, with the experimental results mostly aligning with theoretical expectations derived from these principles. In particular, standard reduction potentials (SRP), which show that the theoretical voltage for a Zn-Cu galvanic cell under standard conditions should approximately be 1.10 V, calculated from the difference in SRPs of Zn and Cu. The SRP value for the Zn^{2+}/Zn cell is -0.76 V, while the SRP value for the Cu^{2+}/Cu cell is +0.34 V. Since the Zn is being oxidised, the SRP is subtracted, thus the theoretical cell voltage $E^\circ = (+0.34) - (-0.76) = 1.10 \text{ V}$ [10], as represented in Table 2.

This theoretical value for voltage was closely represented by the measured voltages for the single cell configurations, which ranged from 1.075 V to 1.077 V depending on the concentration of the electrolyte solutions. The measured V_{oc} had a deviation of less than 2.3% when compared to the theoretical value, reflecting that the experimental setup closely approximated standard reaction conditions

The minimal increase in the voltage as the concentration of the electrolyte increased may be attributed to the Nernst equation, which predicts that increasing ion concentration at the cathode and decreasing ion concentration at the anode will increase the cell potential at non-standard conditions, where a lower value for the reaction quotient Q would result in a larger overall cell potential E [11]. However, while the concentrations of the anode and cathode were increased during the experiment, the concentration of the anode was always the same as the cathode for each trial. Thus, it is likely that the slight increase in voltage across the single half-cells was not due to the effect of the Nernst equation.

The explanation for the increase in voltage could be attributed to increase in the absolute (instead of the relative) concentrations of the Zn^{2+} and Cu^{2+} ions, which enhanced the measured performance of the galvanic cell through the voltage. This is due to real-world electrochemical effects, such as the higher ion concentration improving the availability of ions at the electrode surfaces, which means that there are more ions that can be used up in the redox reaction [12]. This allows the redox reaction to proceed at a faster rate than at a lower concentration, allowing the cell to maintain a higher voltage, especially under load such as when powering the LED light. A greater number of ions in the electrolyte solution also increases the electrolyte's ionic conductivity, which could reduce the internal resistance and help to minimise the voltage

lost across the cell, which maximises the voltage output [13]. However, these effects were likely minimal because the electrolyte solutions were already fairly saturated at all concentrations, hence the relatively low (but measurable) increase in the voltage produced by the cell.

From an engineering perspective, the experimental results demonstrate that increasing electrolyte concentration slightly improves the measured voltage output of the Zn-Cu galvanic cells. While the theoretical voltage based on the Nernst equation should remain constant because the electrolyte concentrations of Zn^{2+} and Cu^{2+} remained equal to one another, the observed increase in voltage at higher concentrations is not due to changes in the potential predicted by the Nernst equation [14] Instead, this reflects real-world improvements in the performance of the electrochemical system; higher ion concentrations enhance ionic conductivity, increase ionic availability for redox reactions and help slightly improve the voltage output. However, even with these improvements, the single half-cells were still unable to produce enough voltage required to power the LED lights, demonstrating the real-world engineering limitations of the galvanic single half-cell design.

4.2 Effect of electrolyte concentration on current

The decrease in current due to the increase in concentration can be attributed to the different physical and chemical reactions that take place due to this oversaturation. These potential changes are likely due to the formation of a thick layer of solid electrolytes over the metal sheets. According to Ohm's law, voltage (V) is equal to current (I) multiplied by resistance (R), as per (6).

$$V = IR. \quad (6)$$

Although increasing the electrolyte concentration generally improves ionic conductivity and reduces internal resistance, a marginal decrease in current was observed at the highest concentration. This may be attributed to non-ideal factors such as increased solution viscosity or concentration polarisation near the electrode surfaces, which can hinder ion mobility. However, within the tested concentration range, these effects are likely minimal, and the slight drop in current could also result from measurement variability or inconsistencies in electrode surface

4.3 Effect of electrolyte concentration on power output

This trend also influenced the specific power and energy of the cells. Specific power, which reflects the rate of energy delivery per unit electrode area, decreased in single-cell setups as concentration increased—again due to reduced current. Specific energy, representing total energy output per unit volume of electrolyte, was not measurable for single cells as they could not power LEDs. This highlights the limitations of relying solely on concentration to enhance performance. While higher concentrations slightly improved voltage due to increased ionic conductivity and ion availability, the overall energy delivery capacity remained limited without further system enhancements.

4.4 Effects of Series Connection on Voltage and LED Activation

According to Kirchhoff's law, the total voltage across the series of cells is determined by the sum of the individual cell voltages [15]. Thus, as each cell produces 1.10 V, two cells in series should produce 2.20 V and three cells in series should theoretically produce 3.30 V. Whilst the individual voltage of a single cell (1.10 V) was insufficient to power any of the LEDs, connecting the cells in series increased the combined voltage, which allowed the system to reach higher voltage thresholds required to power the LEDs [14]. This is shown by Table 3, which demonstrates that two half-cells in series produced voltages of 2.075 V and 2.145 V; this voltage was high enough to power the red LED light, which required a voltage of 2.075 V. However, this was not sufficient to power the other cells, and as such three cells were connected in series, obtaining a voltage of 3.188 V, as seen in Table 3. This allowed the system to successfully power all the LEDs of each colour in decreasing order of voltage from green to red.

To ensure consistent and reliable testing, LEDs were evaluated in decreasing order of their minimum voltage threshold, beginning with the green LED and ending with the red. This approach was selected in order to minimise the risk of current depletion or voltage drop due to the gradual loss of available energy as the galvanic cell is used up over time [16]. Since the higher voltage LEDs (such as green) require greater amounts of energy to light up, testing them first ensured that the system of cells was operating at its maximum available voltage and current output. If the lower voltage LEDs (such as red) had been tested first, the system of cells would have likely experienced a measurable decline in performance due to a depletion of ions or other factors causing a loss in the available energy from the cells, potentially inhibiting the successful light-up of the later LEDs, which have higher voltage thresholds and greater energy requirements. By testing the LEDs from the highest to lowest voltage threshold, the experimental design ensured that the system was able to power the lights with its full energy capacity, without prematurely exhausting its energy potential.

4.5 Analysis of specific power and specific energy

The specific power, measured in mW/cm^2 (although usually measured in power per unit mass) demonstrates how quickly a system can deliver energy to an output, per unit area of the electrode surface [17]. This indicates the rate at which energy can be delivered, as a higher specific power corresponds to more efficient uses of the electrode surface for fast and effective energy delivery to the power output. This can be seen by the higher specific power values in Table 4 for the cells in series, however the specific power decreases as concentration increases for the single half-cells, due to the decrease in the current.

The specific energy, measured in mJ/mL , represents the total amount of energy delivered per unit volume of electrolyte solution. It corresponds to the system's ability to store and release energy over time, rather than the rate of delivery [18]. As seen in Table 4, there were no energy values determined for the single half-cells, as these cells were unable to power any of the LED lights individually, and thus there was no measurable energy that was delivered to a load. The highest specific energy was observed in the configuration with three half-cells in series, reaching $0.4 \text{ mJ}/\text{mL}$, indicating that combining cells not only increases voltage but also enhances the total energy output. Interestingly, while higher electrolyte

concentrations generally improve voltage and current, the specific energy did not increase linearly with concentration. This suggests that beyond a certain point, factors such as internal resistance or ion saturation may limit the efficiency of energy transfer for the system of cells.

The specific energy values were calculated per unit volume of electrolyte; the specific power values were calculated per unit area of the submerged electrode. However, this likely led to inaccuracies with the true value of the specific power, because the area of the submerged electrode was assumed to be 6 m^2 for all the half-cells, leading to inconsistencies that were not considered. This had less effect in the specific energy, as the electrolyte volume was measured using a measuring cylinder, which is much more accurate than a human submerging the electrodes to approximately the same level for each cell. Thus, estimating the electrode submersion depth caused more variability for the surface area calculations and limited the accuracy of the specific power calculations.

4.6 Limitations and future improvements

Despite the overall success of the experimental setup, several limitations may have influenced the accuracy and reliability of the results. One key limitation is electrode fouling, where the accumulation of reaction by-products or solid electrolyte layers on the electrode surfaces can hinder electron transfer and reduce current output [19]. This is particularly relevant at higher electrolyte concentrations, where oversaturation may accelerate such deposition. Another issue is ionic depletion, especially during prolonged operation or repeated testing. As ions are consumed in redox reactions, their local concentration near the electrode surfaces can drop, leading to reduced reaction rates and voltage instability. Additionally, measurement error may have occurred due to inconsistencies in electrode submersion depth [20] manual handling of components, and contact resistance in the alligator clips and wiring. To address these limitations, future experiments could incorporate standardised electrode holders to ensure consistent surface area exposure and stirring systems (or possible flow systems with an electrolyte reservoir) to maintain uniform ion distribution and prevent depletion [21]. Repeating measurements and using statistical analysis would also improve data reliability. Finally, upgrading to low-resistance connectors and more precise instrumentation would help minimise electrical losses and improve the accuracy of voltage and current readings.

4.7 Evaluation of engineering applications

The findings of this investigation have direct applications to real world engineering problems, particularly in areas such as energy efficiency, sustainability and cost effectiveness. Practically, in the design of batteries for devices such as medical implants and portable electronics, it is important to optimise specific power and specific energy in order to deliver reliable performance without excessive inputs of materials or energy. This is particularly important in medical implantable devices such as pacemakers, which need to be small, safe and effective [22]-[23]. Furthermore, in the field of sustainable batteries, electrochemical cells have been used to create rechargeable batteries [24]. While increasing the concentration of electrolytes and linking cells in series improved the voltage, power and energy outputs, this approach is likely not scalable to more intricate and larger

batteries due to the higher cost, environmental impact of high-concentrated solutions and the configurational complexities of cells in series on a large scale. Also, there are likely to be diminishing returns of voltage and power output at higher concentrations, due to the effects of reduced current from increased internal resistance. This demonstrates the importance of understanding the real-world engineering limitations when trying to optimise electrochemical enhancements to the system. This highlights the need for a system design that considers sustainability of materials, manufacturability, longevity of the system, and the reality of real-world conditions in addition to electrochemical performance [25]. These insights can be informed by considerations such as the Nernst equation. However, even considerations such as these are somewhat theoretical, and cannot fully account for discrepancies in real-world systems.

5. Conclusion

The study demonstrated the significant impact of electrolyte concentration and cell configuration on the performance of Zn-Cu galvanic cells. Connecting three half-cells in series yielded the highest performance, achieving 3.19 V, 1.67 mA, and 15.98 mJ of energy output (refer to Table 2 and Table 3). In contrast, individual cells (~1.1V) were unable to power even the lowest-threshold LED, underscoring the importance of voltage summation in series connections. These findings illustrate the importance of both chemical environment and system arrangement in optimising electrochemical performance. Significant trade-offs existed between simplicity of setup and the voltage required to power more highly demanding electronic components. While elevated electrolyte concentrations improve performance, practical applications must balance this with considerations such as cost, stability, and environmental safety of concentrated solutions.

A valuable direction for future research would be to investigate the effects of alternative electrolyte compositions, such as biodegradable or polymer-based solutions, which may enhance sustainability while maintaining sufficient ion conductivity and redox activity over repeated cycles.

Authorship

The outlined investigation was conducted and performed by all authors. Anastasiia Danshyna completed all formatting for data visualisation tables (Tables 1-3) and figures (Figures 1-5), contributed to results section 3.1, wrote the conclusion, and carried out the full formatting and structuring of the article. Grace Mihaljevic completed the methods and equipment sections, and contributed to Tables 1-3, and Figures 1-5. Stefano Furlan completed the discussion section (4.1, 4.3-4.7), interpreting results through electrochemical engineering principles. Isaac Sleath completed the abstract and introduction sections. Alexander Palmer completed the discussion section (4.2), interpreting the effects of oversaturation on galvanic cells and the connection of batteries in a series in relation to Kirchhoff's law. Tutors (Masoomah Asghar Nejad-Laskoukalayeh, Jordan Kambanis and Benedict Tai,) provided task direction and project assistance, Dr Thomas Whittle designed the experiment, Dr David Alam facilitated project resources and guidance on conceptual direction, and Dr. Gobinath Rajarathnam ideated

conceptual direction, research and writing guiding frameworks, and direct project supervision.

Acknowledgements

The authors acknowledge the limited use of generative artificial intelligence (ChatGPT) to support the writing of this article. However, all the report's content was developed independently by the authors.

References

- [1] G. Li *et al.*, "Developing Cathode Materials for Aqueous Zinc Ion Batteries: Challenges and Practical Prospects," *Advanced Functional Materials*, vol. 34, no. 5. 2024. doi: 10.1002/adfm.202301291.
- [2] M. Al-Amin, S. Islam, S. U. A. Shibly, and S. Iffat, "Comparative Review on the Aqueous Zinc-Ion Batteries (AZIBs) and Flexible Zinc-Ion Batteries (FZIBs)," *Nanomaterials*, vol. 12, no. 22. 2022. doi: 10.3390/nano12223997.
- [3] B. Tang, L. Shan, S. Liang, and J. Zhou, "Issues and opportunities facing aqueous zinc-ion batteries," *Energy and Environmental Science*, vol. 12, no. 11. 2019. doi: 10.1039/c9ee02526j.
- [4] Z. Salameh, *Renewable Energy System Design*. 2014. doi: 10.1016/C2009-0-20257-1.
- [5] Battery lab instructions. Preparation and Testing of Galvanic Cells Using Copper and Zinc Electrodes. 2025. *USYD CBE Materials*.
- [6] H. Zhang *et al.*, "Using Li+ as the electrochemical messenger to fabricate an aqueous rechargeable Zn-Cu battery," *Chemical Communications*, vol. 51, no. 34, 2015, doi: 10.1039/c5cc00575b.
- [7] A. Jameson, A. Khazaeli, and D. P. J. Barz, "A rechargeable zinc copper battery using a selective cation exchange membrane," *Journal of Power Sources*, vol. 453, 2020, doi: 10.1016/j.jpowsour.2020.227873.
- [8] G. P. Rajarathnam and A. M. Vassallo, "The Zinc/Bromine Flow Battery," *SpringerBriefs in Energy*, 2016.
- [9] Feiner, A. S., & McEvoy, A. J. (1994). The nernst equation. *Journal of chemical education*, 71(6), 493.
- [10] C. Shin, L. Yao, S. Y. Jeong, and T. N. Ng, "Zinc-copper dual-ion electrolytes to suppress dendritic growth and increase anode utilization in zinc ion capacitors," *Sci. Adv.*, vol. 10, no. 1, Art. no. eadf9951, Jan. 2024, doi: 10.1126/sciadv.adf9951.
- [11] L. Wen *et al.*, "Effect of composite conductive agent on internal resistance and performance of lithium iron phosphate batteries," *Ionics*, vol. 28, no. 7, pp. 3145–3153, 2022.
- [12] Y. S. Hu, Y. Lu, "The Mystery of Electrolyte Concentration, from Superhigh to Ultralow," *ACS Energy Lett*, vol. 5, no. 11, pp. 3633-3636, 2020 <https://pubs.acs.org/doi/full/10.1021/acsenerylett.0c02234> (12)
- [13] L. Liu, J. Zhu, and L. Zheng, "An effective method for estimating state of charge of lithium-ion batteries based on an electrochemical model and Nernst equation," *IEEE Access*, vol. 8, pp. 211738–211749, 2020.
- [14] R. Drummond, L. D. Couto, and D. Zhang, "Resolving Kirchhoff's laws for parallel li-ion battery pack state-

estimators," *IEEE Trans. Control Syst. Technol.*, vol. 30, no. 5, pp. 2220–2227, 2021.

[15] K. Lacina, J. Sopoušek, P. Skládal, and P. Vanýšek, "Boosting of the output voltage of a galvanic cell," *Electrochimica Acta*, vol. 282, pp. 331–335, 2018.

[16] L. Redley, "Lithium batteries for pulse power," presented at the 10th Annual Battery Conf. on Applications and Advances, Long Beach, CA, USA, 1990. [Online]. Available: <https://www.osti.gov/servlets/purl/6118809-p2HtVA/>

[17] P. M. Biesheuvel, M. van Soestbergen, M. Z. Bazant, "Imposed currents in galvanic cells," *Electrochimica Acta*, vol. 54, no. 21, pp. 4857–4871, 2009. <https://doi.org/10.1016/j.electacta.2009.03.073>

[18] R. V. Kumar and T. Sarakonsri, *Introduction to Electrochemical Cells, in Rechargeable Ion Batteries*, Singapore: Springer, 2022.

[19] B. L. Hassen, S. Siraj, D. K. Y. Wong, "Recent strategies to minimise fouling in electrochemical detection systems," *Reviews in Analytical Chemistry*, vol. 35, no. 1, 2016. <https://www.degruyterbrill.com/document/doi/10.1515/revac-2015-0008/html#APA>

[20] P. Vanýšek, "Impact of electrode geometry, depth of immersion, and size on impedance measurements," *Canadian Journal of Chemistry*. 1997, <https://doi.org/10.1139/v97-194>.

[21] Gunawan *et al.* "Energy storage system from galvanic cell using electrolyte from a plant as an alternative renewable energy," *IOP Conf. Series: Material Science and Engineering*, 2019, doi:10.1088/1757-899X/509/1/012045.

[22] D. C. Bock, A. C. Marschilok, K. J. Takeuchi, and E. S. Takeuchi, "Batteries used to power implantable biomedical devices," *Electrochimica Acta*, vol. 84, pp. 155–164, 2012, doi: [10.1016/j.electacta.2012.03.057](https://doi.org/10.1016/j.electacta.2012.03.057).

[23] R. Latham, R. Linford, W. Schlindwein, "Biomedical applications of batteries," *Solid State Ionics*, vol. 172, no. 1-4, pp. 7-11, 2004 <https://doi.org/10.1016/j.ssi.2004.04.024>.

[24] S. Mypati, A. Khazaeli, D. P. J. Barz, "A novel rechargeable zinc-copper battery without a separator," *Journal of Energy Storage*, vol 42, 2021, <https://doi.org/10.1016/j.est.2021.103109>

[25] L. B. Wheeler, B. A. Whitworth, A. L. Gonczi, "Engineering design challenge: building a voltaic cell in the high school chemistry classroom," *The Science Teacher*, vol. 81, no. 9, pp. 30-36, 2014, https://doi.org/10.2505/4/tst14_081_09_30